PERFORMANCE OF OSCILLATING CONVEYORS

Sabry A. El-Shakery, Raafat A. Abou Elnasr and Khalid M. Khidr
Production Engineering and Design Department
Faculty of Engineering, Menoufia University
Shebin ElKom, Egypt

ABSTRACT

This work presents the analysis for the performance of oscillating conveyors. Two types are considered namely, the variable pressure and the constant pressure types of conveyors. Equations of motion were derived and the solution yields the conveying capacity. An experimental model for the first type was constructed for verifying the analytical analysis. Both experimental and analytical results came in good agreement. The study was completed by determining the effect of all parameters on the conveying capacity.

NOMENCLATURE

g Gravity acceleration
m Mass of the conveyed particle.
N Normal reaction force on the trough.
Q Conveying capacity.
q Conveying advance per cycle.
r Link length.
S Displacement integration constant.
t Time.
V Velocity integration constant.
μ Coefficient of friction (dynamic μ_d or static μ_s).
X,Y,x,y: Global and trough point coordinates.
ϕ Angular displacement of link.
ω Angular speed.
α Angular acceleration.
ψ Conveyability factor.

Subscripts

$()_i$ Number of link or integrating constant.
$()_L$ Load.
$()_L$ Lower value.
$()_r$ Relative value.
$()_{ri}$ Initial relative value.
$()_s$ Stroke.
$()_t$ Trough.
$()_U$ Upper value.

INTRODUCTION

The performance of the oscillating conveyors is measured by the conveying capacity per operating cycle. A few and incomplete analysis to design such conveyors have been reported in [1-8]. The general characteristics of such conveyors have been explained in [1,2]. The analysis of the trough motion, which is driven by an eccentric cam has been presented in [3]. Moreover, an analysis considering the trough motion to be parabolic has been carried out in [4]. The analysis of a single particle motion has been presented in [5,6], the particle motion was considered to be any one of the following different forms which are sliding along, riding on, or flying above the trough. In addition, in [7], the vibrotransport conditions are chosen such that the motion of bulk material proceeds without any relative slipping and the average speed of the motion would be determined mainly by movement of the charge in the flight stage. A computer aided design method has been presented in [8] for determining the performance of various mechanisms which are used to drive such conveyors. It has been concluded that the four-bar mechanism is suitable to drive such conveyors. Consequently, this paper is concerned with the study of the performance of the oscillating conveyors. complete analytical motion analysis for obtaining the conveying advance or the conveying capacity.

DESCRIPTION ON THE SYSTEMS

Figure (1) shows the investigated systems, which are type I conveyor with variable pressure on the trough bed and type II conveyor with constant pressure. Each conveyor is driven by two four link mechanisms in series.

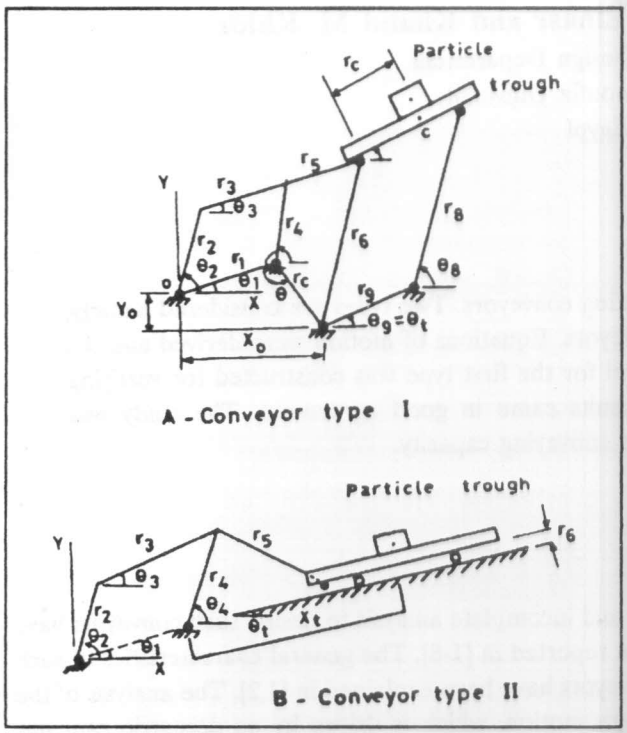

Figure 1.

ANALYTICAL ANALYSIS

Equations Of The Load Motion

The load is represented by a particle moving relative to the trough surface as shown in Figure (2).

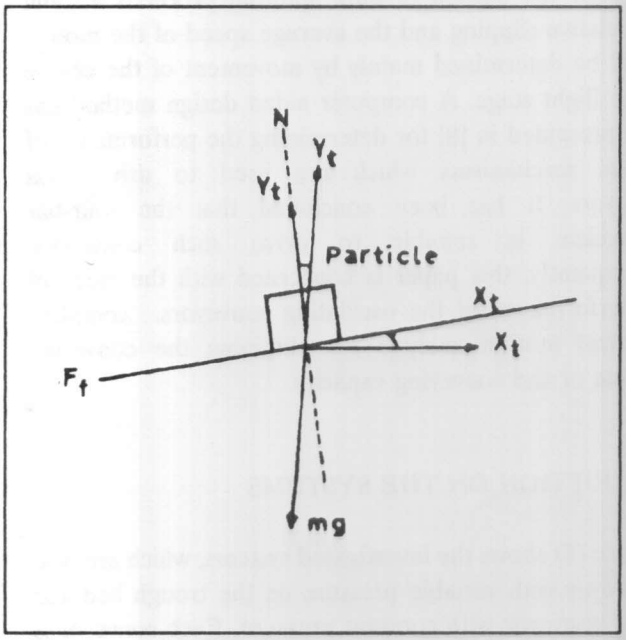

Figure 2.

The components of the particle acceleration $\ddot{x}_l$, $\ddot{y}_l$ are given by:

$$\ddot{x}_l = \ddot{x}_t + \ddot{x}_r \qquad (1)$$

$$\ddot{y}_l = \ddot{x}_t + \ddot{y}_r$$

where $\ddot{x}_t$ and $\ddot{y}_t$ are the components of the trough acceleration and are given by:

$$\ddot{x}_t = \ddot{X}_t \cos\theta_t + \ddot{Y}_t \sin\theta_t \qquad (2)$$

$$\ddot{y}_t = \ddot{Y}_t \cos\theta_t - \ddot{X}_t \sin\theta_t$$

The general equations of the particle motion are in the form:

$$m\,\ddot{x}_l + mg \sin\theta_t + u\,N\,\mathrm{sgn}(\dot{x}_r) = 0 \qquad (3)$$

$$m\,\ddot{y}_l + m\,g\cos\theta_t - N = 0$$

where the normal reaction force N is given by:

$$N = m\,\ddot{y}_l + m\,g\cos\theta_t \qquad (4)$$

The relative motion between the load particle and the trough bed undergo the following stages:

Pure Riding Stage

In this stages, there is no relative motion. This condition occurs when $N > 0$ and $|B_o| \leq u_s |A_o|$
Where:

$$B_o = m\,\ddot{x}_l + mg \sin\theta_t \qquad (5)$$

$$A_o = m\,\ddot{y}_l + mg\cos\theta_t$$

In this case,

$$y_r = \dot{y}_r = \ddot{y}_r = \dot{x}_r = \ddot{x}_r = 0$$

Also x_r is constant and is equal to the value of x_r at the initial position of this stage (x_{ri}).

Sliding Stage

In this case, the normal relative motion to the trough is

zero ($y_r = \dot{y}_r = \ddot{y}_r = 0$). This stage occurs when

$$N > 0 \quad \text{and} \quad |B_o| > u_s |A_o|$$

Hence the equation of the particle motion is in the form,

$$m \ddot{x}_t + mg \sin\theta_t + \text{sgn}(\dot{x}_r)\, u_d N = 0 \qquad (6)$$

Substituting equations (1) and (4) into equation (6), the relative acceleration component $\ddot{x}_r$ can be determined by:

$$\ddot{x}_r = C_o + u_d K \ddot{y}_t - \ddot{x}_t \qquad (7)$$

By integrating equation (7), the components of relative velocity and displacement $\dot{x}_r$ and x_r can be estimated by:

$$\dot{x}_r = C_o t + u_d K \dot{y}_t - \dot{x}_t + V_1 \qquad (8)$$

and

$$x_r = (C_o/2)t^2 + u_d K y_t - x_t + V_1 t + S_1$$

where:

$$K = -\text{sgn}(\dot{x}_r), \quad C_o = g(u k \cos\theta_t - \sin\theta_t),$$

$$V_1 = -C_o t - u k \dot{y}_t + \dot{x}_t + \dot{x}_{ri} \text{ and}$$

$$S_1 = -C_o (t^2/2) - u k y_t + x_t - V_1 t + x_{ri}$$

Flight Stage

In this stage, the contact between the particle and trough is lost. Hence the equations of motion are given by:

$$m \ddot{x}_t + mg \sin\theta_t = 0 \qquad (9)$$

$$m \ddot{y}_t + mg \cos\theta_t = 0$$

Using equation (1), the relative acceleration components $\ddot{x}_r$ and $\ddot{y}_r$ are given by:

$$\ddot{x}_r = -\ddot{x}_t - g \sin\theta_t$$

$$\ddot{y}_r = -\ddot{y}_t - g \cos\theta_t \qquad (10)$$

Consequently,

$$\dot{x}_r = -\dot{x}_t - gt \sin\theta + V_2 \qquad (11)$$

$$\dot{y}_r = -\dot{y}_t - gt \cos\theta_t + V_3$$

and

$$x_r = -x_t - g(t^2/2) \sin\theta_t + V_2 t + S_2$$

$$y_r = -y_t - g(t^2/2) \cos\theta_t + V_3 t + S_3 \qquad (12)$$

Where

$$V_2 = \dot{x}_t + gt \sin\theta_t + \dot{x}_{ri}, \quad V_3 = \dot{y}_t + g t \cos\theta_t + \dot{y}_{ri}$$

$$S_2 = x_t + g(t^2/2) \sin\theta_t - V_2 t + x_{ri}$$

$$S_3 = y_t + g(t^2/2) \cos\theta_t - V_3 t + y_{ri}$$

It should be noted that, the initial values of each stage are equal to the final values of the preceding stage. The motion over the whole cycle is carried out according to the flow chart shown in Figure (3).

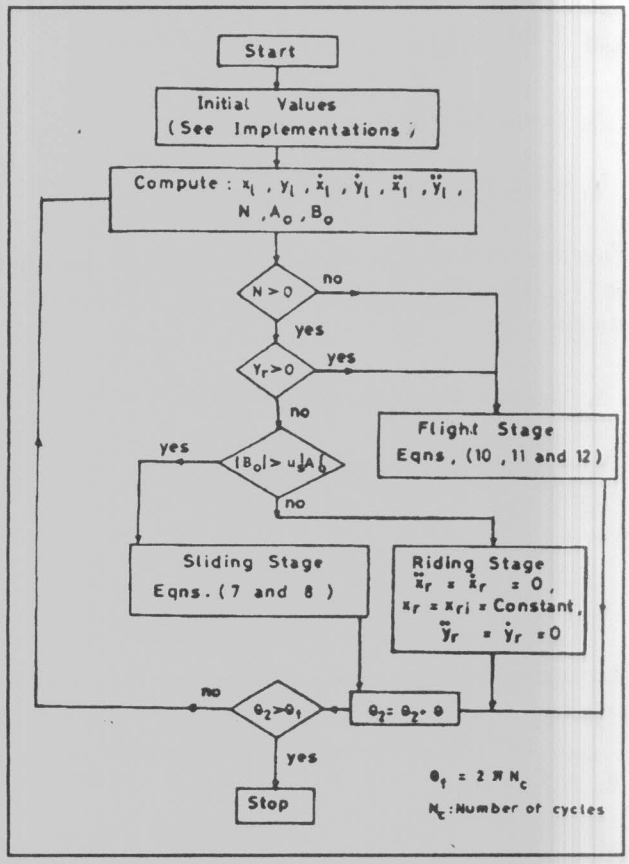

Figure 3. Flow chart.

The value of x_r at the end of the cycle represents the

amount of the conveying advance per cycle and is denoted by q. x_t and y_t depend upon the conveyor type as follows:

Motion Analysis of Conveyors

For Variable Pressure Conveyor (Type I):

From the analysis of such conveyor, the global coordinates X_t and Y_t can be derived according to Figure (1), as

$$X_t = r_{c7} \cos \theta_t + r_6 \cos \theta_6 + X_o$$
$$Y_t = r_{c7} \sin \theta_t + r_6 \cos \theta_6 + Y_o \quad (13)$$

Hence, by differentiation, we obtain:

$$\dot{X}_t = - r_6 \omega_6 \sin \theta_6$$
$$\dot{Y}_t = r_6 \omega_6 \cos \theta_6 \quad (14)$$

and

$$\ddot{X}_t = - r_6 (\theta_6)^2 \cos \theta_6 + \alpha_6 \sin \theta_6$$
$$\ddot{Y}_t = - r_6 (\theta_6)^2 \sin \theta_6 - \alpha_6 \cos \theta_6 \quad (15)$$

Equations (13) to (15) are used to solve equations (2), (7) and (8). The stroke components (X_s and Y_s) of the trough are given by:

$$X_s = r_6 [\cos (\theta_6)_L - \cos (\theta_6)_U]$$
$$Y_s = r_6 [\sin (\theta_6)_U - \sin (\theta_6)_L] \quad (16)$$

Where

$$Y_s = r_6 [1 - \sin (\theta_6)_L] \text{ for } \theta_6 > 90^\circ$$

The corresponding angular positions of the crank are given by:

$$\theta_{2L} = \theta_1 + \phi_1$$

and (17)

$$\theta_{2U} = \theta_1 + \phi_2$$

where:

$$\phi_{1,2} = \cos^{-1} [r_1^2 + (r_3 \pm r_2)^2 - r_4^2]/[2r_1 (r_3 \pm r_2)]$$

For Constant Pressure Conveyor (Type II):

The analysis of this conveyor implies the following:

$$x_t = r_4 \cos (\theta_4 - \theta_t) + r_5 . A_c$$
$$y_t = r_6 = \text{offset amount} \quad (18)$$

By differentiation, we obtain:

$$\dot{x}_t = r_4 \omega_4 \sin (\theta_4 - \theta_t) + r_5 . \dot{A}_c$$
$$\ddot{x}_t = -r_4[\alpha_4 \sin(\theta_4 - \theta_t) + \omega_4 \cos(\theta_4 - \theta_t)] + r_5 . \ddot{A}_c \quad (19)$$

and

$$\dot{y}_t = \ddot{y}_t = 0.0$$

These equations are used for solving equations (2),(7) and (8). The tough stroke components (X_s, Y_s) are:

$$X_s = x_{tU} - x_{tL}, \quad Y_s = X_s \tan \theta_t \quad (20)$$

Where x_{tU} and x_{tL} are determined at the extreme positions of the crank, equation (17).

The kinematic analysis of the driving mechanism is given in the Appendix.

CONVEYING CAPACITY

The conveying capacity per operating cycle Q for such conveyors is proportional with the conveying advance q and is expressed as:

$$Q = \psi . q \quad (21)$$

EXPERIMENTAL WORK

An experimental model for type I conveyor was constructed to measure the relative displacement between the conveyed particles and the trough. A cubic wooden specimen with a 5cm side is used as a particle. A scaled paper is fixed on the trough side to measure the relative motion of the specimen.

The equipment

- Stroboscope (to measure the crank-shaft speed),
- Video camera (sharp 500 S),
- Video device (National - G 220 - digital), and
- T.V. (National 20 inches).

The results of this test and the corresponding theoretical one are plotted in Figure (4).

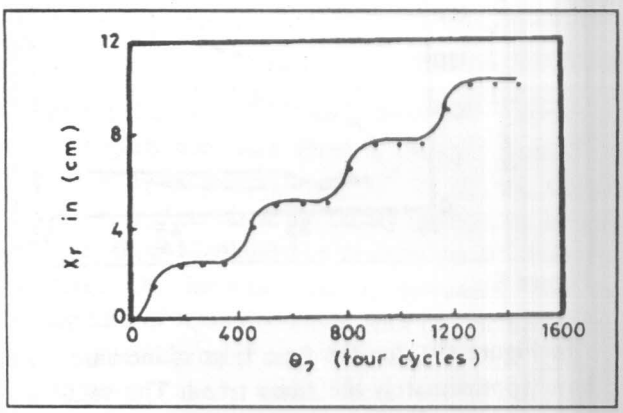

Figure 4. __ Measured relative displacement .... theoretical relative displacement with the following initial values:

r_1 = 35 cm, r_2 = 3 cm, r_3 = 47 cm, r_4 = 41.5 cm, r_5 = 39.5 cm, r_6 = 49.5 cm, r_7 = 43.5 cm, u = 0.634, ω_2 = 1.3 rad/sec, $\theta_1 = \theta_c = \theta_t = 0$.

Figure (4) indicates that, the measuring values of the relative displacement x_r during four operating cycles of crank is in considerable agreement with the theoretical ones which were computed at the same initial values.

IMPLEMENTATIONS

The computer program is implemented with the following initial data:

r_1 = 100cm, r_2 = 40cm, r_r = 153cm, r_c = 135cm, r_5 = 240cm, r_6 = 250cm, r_c = 70cm, X_o = 170cm, Y_o = 0, r_9 = 300cm, u = u_s = u_d = 0.3, ω_2 = 4.5 rad/sec, $\theta_1 = \theta_c = \theta_t = 0$, T_r = 1.52, $x_r(0) = \ddot{x}_r(0) = 0$, $y_r(0) = \dot{y}_r(0) = \ddot{y}_r(0) = 0$.

The value of r_6 is considered equal to zero for type II conveyor.

RESULTS AND DISCUSSIONS

For Type I Conveyor

Figure (5-A) indicates that, the positive sliding, riding, negative sliding and flight stages occurred in order. It is clear that the most of the advance is gained during the flight and negative sliding stages. Figure (5-B) shows the path of the load particle while figure (5-C) indicates the relative displacement components.

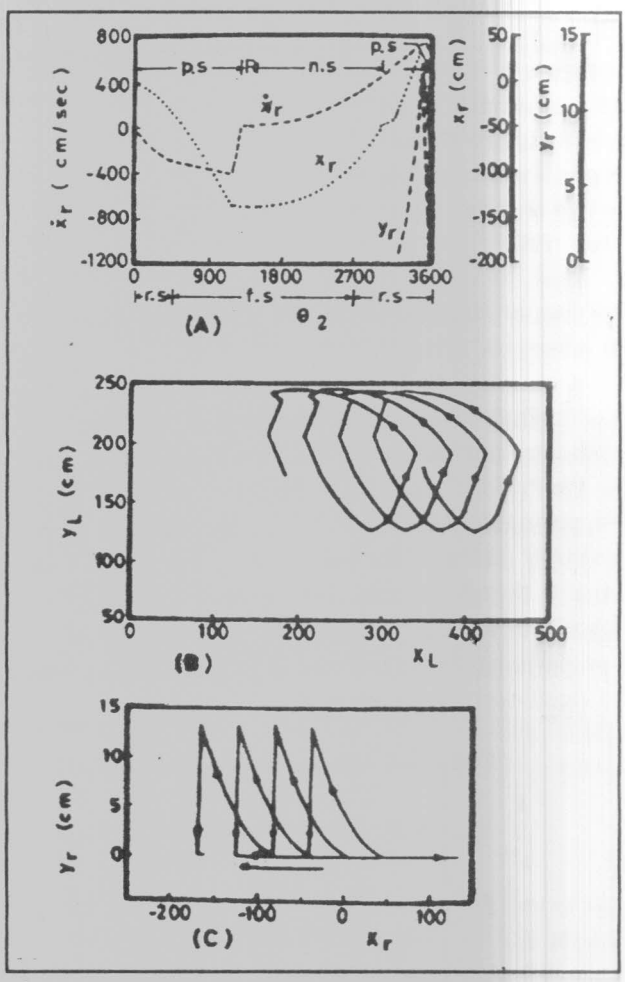

Figure 5.

For Type II Conveyor

In this type there is no occurrence of flight mode. In

Figure (6), the positive sliding period is greater than that of the negative sliding one and x_r increases in (↑R) more than its increase in (↑F). Hence the particle is conveyed in (↑R).

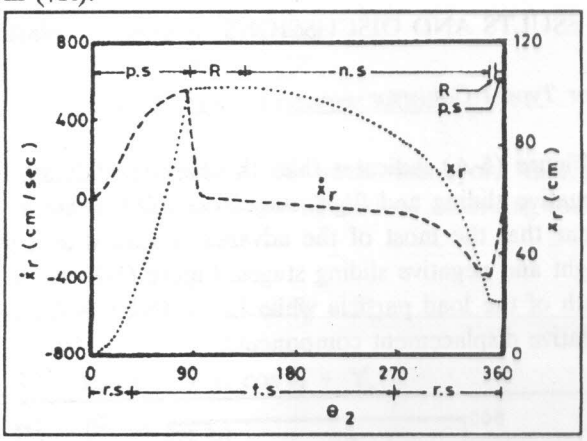

Figure 6.
f.s : Forward stroke,
r.s : Return stroke
p.s : Positive sliding
n.s : negative sliding
R : Riding

Effect of Parameters On The Conveying Advance

A complete study has been made to determine the effect of driving mechanism parameters on the conveying advance and the trough stroke components X_s and Y_s.

For type I conveyor, Fig. (7) indicate that, X_s is approximately constant and Y_s decreases as r_1 increases. Also, q increases for values of r_1 less than 93 cm, after that it slightly decreases. For type II conveyor, X_s is little sensitive to the variation in r_1, while q is inversely proportional to the increase in r_1. Hence, increasing r_1 has a significant influence on X_s.

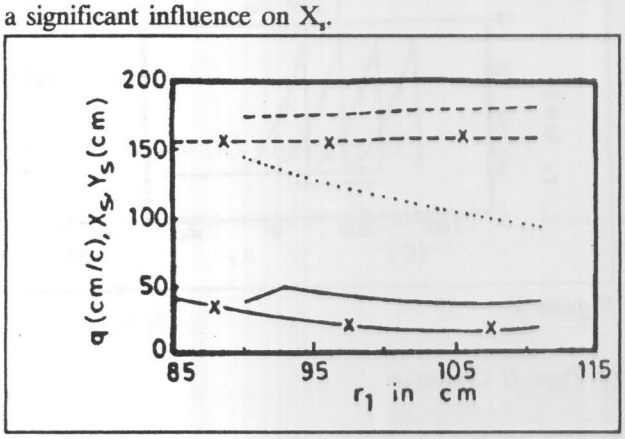

Figure 7.

Figure (8) shows that, for type I, as r_2 increases, both X_s and Y_s increase considerably. Also, q decreases and then slightly increases. Accordingly, the value of r_2 should be more than 40cm. For type II, increasing r_2 results in continuous increase in X_s and also q is influenced with increase in r_2. This influence varies and increases for r_2 greater than 40cm. Therefore r_2 should be more than 44cm.

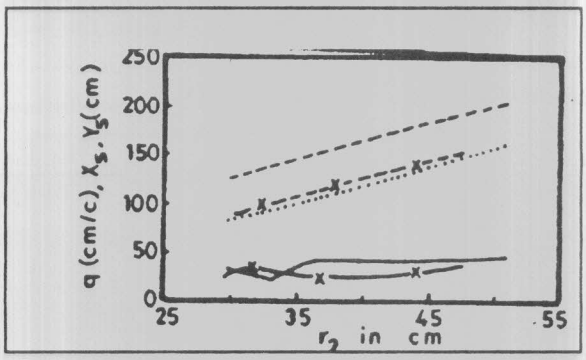

Figure 8.

In Figure (9), for the type I, as r_3 increases, q and Y_s have approximately the same trend. The value of X_s are independent of r_3. In order to increase q, r_3 should be increased within the considered limits. For type II, as r_3 increases, with a constant rate, while q is affected by any variation in r_3 as shown. It seems that the maximum value of q occures when r_3 is about 140cm or a little less.

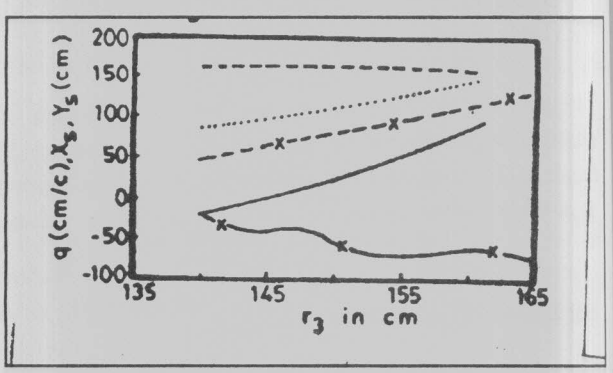

Figure 9

In Figure (10), for type I conveyor, as r_4 increases, q and Y_s decrease large while X_s slightly increases. For type II, q increases when r_4 is larger than 140cm.

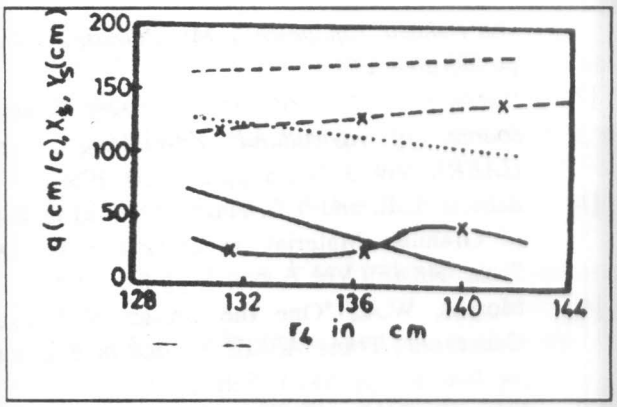

Figure 10.

In Figure (11), for type I, as θ_1 increases q decreases and then slightly increases when θ_1 changes from 5° to 10°. Also, as θ_1 increases from -10° to 10°, X_s slightly increases and Y_s decreases. To satisfy an increase in both q and X_s, θ_1 should be less than or equal to 10°. For type II conveyor, X_s increases as θ_1 increases, but the increasing rate of X_s in decreased with the increase of θ_1. q has irregular changes as θ_1 increases ($-15° \leq \theta_1 \leq 10°$). Moreover, as θ_1 varies from 0.0 to 10°, q is significantly increased.

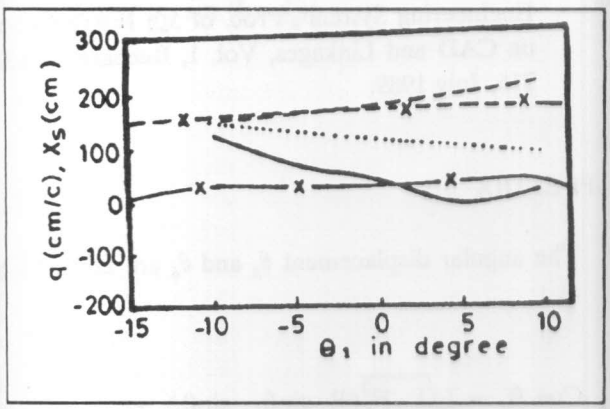

Figure 11.

In Figure (12), for type I, as θ_t increases, q is increased. Also the variation in either X_s or Y_s is not influenced by the variation in θ_t. While for type II conveyor, as θ_t increases positively, q decreases and X_s increases. But with increasing θ_t in the negative direction, q increases and X_s decreases.

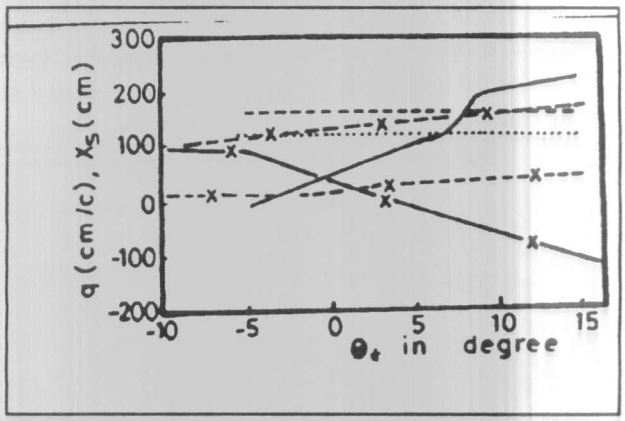

Figure 12.

Figure (13) indicates that, for type I conveyor, q increases with different rates as ω_2 continuously increases and in this case ω_2 should be increased to more than 4.8 rad/s. While for type II, X_s is not influenced by ω_2 and q is significantly influenced by ω_2. Therefore, for a maximum q, ω_2 should bee within $3.5 \leq \omega_2 \leq 3.8$ rad/s. But if ω_2 increases to more than 3.8 rad/s, q will rapidly decreases.

- $\ddot{X}_r$ is changed markedly as shown by the full line.
- Comparison between Figures (4) and (5) confirms the agreement between the relative motion and modes of particle motion.

For the Type II conveyor, we find only three modes of the particle motion, positive sliding, riding and negative sliding modes as shown in Figure (6). There is no occurrence of flight mode, and it is obvious that the sum of positive sliding in direction of the return stroke is greater than the sum of negative one. Hence the particle is coneyed in direction of the return stroke and that the periods of each mode are as follows:

- $0 \leq \theta_2 \leq 88°$ and $354° \leq \theta_2 \leq 360°$ for positive sliding mode,
- $88° \leq \theta_2 \leq 115°$ and $352° \leq \theta_2 \leq 354°$ for riding mode, and
- $115° \leq \theta_2 \leq 352°$ for negative sliding mode.

Comparing this figure with the corresponding one of the Type I conveyor, it can be easily seen that: a) flight modes often occurs in the Type I conveyor, and b) the direction of the particle conveyance in Type I conveyor is opposite to that Type II conveyor. To obtain sufficiently detailed picture of modes of the relative load particle motion to trough, ΣX_r and its differentiation with respect to time are plotted in Figure (7). It is easily noted that ΣX_r is always

in direction of return stroke, this means that the conveying direction is opposite to that in Type I conveyor. Probably this is due to increasing $\ddot{X}_r$ in direction of forward stroke or by decreasing one or all of, r_1, r_4 and θ_1.

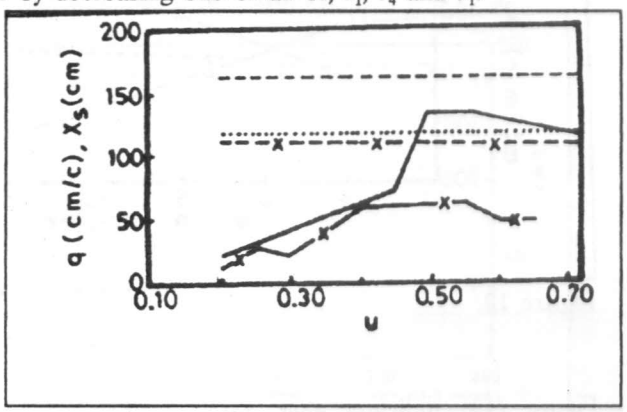

Figure 13.

- Conveying capacity of type II conveyor can be increased by increasing r_2, r_4, θ_1 and u or decreasing r_1, r_3 and θ_t.
- To decrease the stroke components Y_s, for type I conveyor, θ_1, r_1 and r_4 should be increased and r_2 and r_4 should be decreased, while for type II conveyor, θ_t should be decreased.
- Either u or ω_2 plays an important role in determining the conveying capacity and the conveyance direction.
- Such systems may be optimized and or synthesized, using [9], for one or multi-objective functions. The solution of such optimization problem for maximum conveying capacity and its sensitivity formulation will be done in our next work.

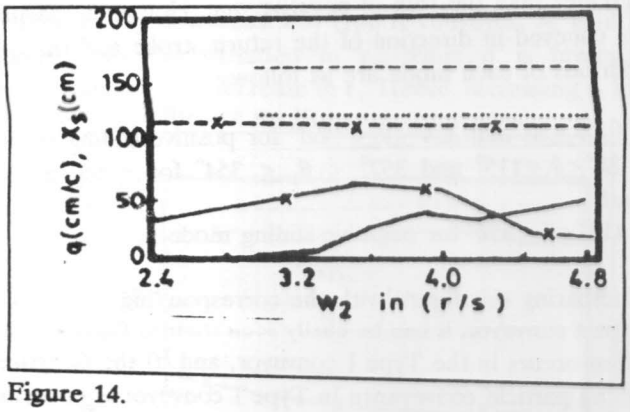

Figure 14.

REFERENCES

[1] Spivakovsky, A. and Dyachokov V., " *Conveyors and Related Equipment*", Mir Publisher, Moscow, pp 295-311, 1968.

[2] Borry, P.E., Research on Oscillating Conveyors', *Journal of Agricultural Engineering Research (JAER)*, Vol. 3, No. 3, pp 249-259, 1958.

[3] Schertz, C.E. and T.E. Hazen, "Predicting Motion of Granular Material on Oscillation Conveyor', *Trans. ASAE*, Vol. 6, No. 1, pp 6-10, 1963.

[4] Morcos, W.A., "One the Design of Oscillating Conveyors", Trans. ASME, *Journal of Engineering for Industry*, pp 53-61, Feb. 1970.

[5] Gaberson, H.A., "Particle Motion on Oscillating Conveyors Part I", *ASME, Journal of Engineering for Industry*, pp 50-56, Feb. 1972.

[6] Gaberson, H.A., "Particle Motion on Oscillating Conveyors Part II", *ASME, Journal of Engineering for Industry*, pp 57-63, Feb. 1972.

[7] Belkov, N.I. et al., "Oscillating Conveyors", *Russian Engg. Journal*, Vol. 58, No. 1, pp 38-40, 1978.

[8] Ferguson, J.M. et al., "Computer Aided Design of Drive Mechanisms for Large Oscillating Conveyors". *Trans. Institution of Engineers Australia*, pp 28-52, 1979.

[9] El-Shakery, S.A., "CAS Design Procedure for an Engineering System", Proc. of 5th IFROMM Sym. on CAD and Linkages, Vol. 1, Bucharest, pp 205-216, July 1989.

APPENDIX

1. The angular displacement θ_4 and θ_6 are derived to be as :

$$\begin{aligned} \text{Cos}\,\theta_p &= [\sqrt{1-F_p^2}(R_m\sin\theta_j - \sin\theta_i) + \\ &\quad F_p(R_m\cos\theta_j - \cos\theta_i)]/A_k \\ \text{Sin}\theta_p &= [F_p(R_m\sin\theta_j - \sin\theta_i) - \\ &\quad \sqrt{1-F_p^2}(R_m\cos\theta_j - \cos\theta_i)]/A_k \end{aligned} \qquad (A.1)$$

Where

$$F_p = (A_k^2 - R_n^2 + R_z^2)/(2R_zA_k)$$
$$A_k = \sqrt{1 + R_m[R_m - 2\cos(\theta_j - \theta_i)]}$$
$$R_m = r_j/r_i, R_n = r_k/r_i, R_z = r_p/r_i$$

Equations (A-1) are used to compute the value of θ_p corrresponding to θ_j.

For (θ_4) put, i = 1, j = 2, k = 3, p = 4, m = 2, n = 3, z = 4

For (θ_6) put, i = c, j = 4, k = 5, p = 6, m = 5, n = 6 , z = 7

Where : subscripts i, j, k and p denote the number of the links.

2. The angular velocities ω_4 and ω_6 are given by:

$$\omega_k = - (r_j/r^{bk})\, \omega_j \, [\sin (\theta_p - \theta_j)/\sin (\theta_p - \theta_k)]$$

$$\omega_p = (r_j/r_p)\, \omega_j \, [\sin (\theta_k - \theta_j) / \sin (\theta_k - \theta_p)] \qquad (A.2)$$

Equation (A.2) are used to compute the value of the angular velocities of links 4 and 6 as follows:

For ω_4 put, i=1 , j=2, k=3, p=4

For ω_6 put, i=c, j=4, k=5, p=6

Where: c for link r_c (see Figure (1-A).

3. Angular accelerations α_4 and α_6 are given by:

$$\alpha_k = B_k / [r_k \sin (\theta_p - \theta_k)]$$

$$\alpha_p = B_p / [r_p \sin (\theta_k - \theta_p)]$$

where:

$$B_k = r_k \omega_k^2 \cos (\theta_p - \theta_k) - r_{jj} \sin (\theta_p - \theta_j) + r_j \omega_j^2 \cos (\theta_p - \theta_j) - r_p \omega_p^2.$$

$$B_p = r_j \alpha_j \, \text{ssin} \, (\theta_k - \theta_j) - r_j \omega_j^2 \cos (\theta_k - \theta_j) + r_p \omega_p^2 \cos (\theta_k - \theta_p) - r_k \omega_k^2 \qquad (A.3)$$

For (α_4) put, i=1, j=2, k=3, p=4

For (α_6) put, i=c, j=4, k=5, p=6

4. For equations (18) and (19) A_c, $\dot{A}_c$ and $\ddot{A}_c$ are given by:

$$A_c = \sqrt{1 - B_c^2} \qquad (A.4)$$

where:

$$B_c = (r_4/r_5) \sin (\theta_4 - \theta_U)) - (r_6/r_5),$$

$$\dot{A}_c = - (B_c \dot{B}_c)/A_c,$$

$$\ddot{A}_c = - A_c (B_c B_c + \dot{B}_c^2) + (B_c \dot{B}_c) \dot{A}_c / A_c^2$$

$$\dot{B}_c = (r_4/r_5) \omega_4 \cos (\theta_4 - \theta_U)$$

$$\ddot{B}_c = (r_4/r_5) - \omega_4^2 \sin (\theta_4 - \theta_U) + \alpha_4 \cos (\theta_4 - \theta_U)$$